

First-principles design of magnetic anisotropy in nanostructures by electric-field, strain, and metal alloying

メタデータ	言語: eng 出版者: 公開日: 2020-01-08 キーワード (Ja): キーワード (En): 作成者: メールアドレス: 所属:
URL	http://hdl.handle.net/2297/00056467

This work is licensed under a Creative Commons Attribution-NonCommercial-ShareAlike 3.0 International License.



Abstract

First-principles design of magnetic anisotropy in nanostructures by electric-field, strain, and metal alloying

電界、ひずみ、合金化によるナノ構造磁気異方性の第一原理設計

Graduate School of
Natural Science & Technology
Kanazawa University

Division of Mathematical and Physical Sciences

Student ID: 1624012010
Name : Indra Pardede
Chief Advisor : Prof. Tatsuki ODA
Date of Submission : June 2019

Abstract

The control of magnetic properties such as magnetic anisotropy (MA) has been intensely pursued during the past few decades. Recently, it has been shown that MA can be controlled by electric field effect and hence shows a great potential to impact in spintronic applications. In this dissertation, we investigated the alloying, strain and EF effect to the magnetic anisotropy energy (MAE) in the structure of which contains Fe/MgO interface with Cr underlayer based on the first principles electronic structure calculations. We found that introducing alloying Fe/Cr can promote the perpendicular MAE (PMAE) in Cr/Fe/MgO structure. Furthermore, the different alloying conditions can lead to the opposite change in the electric field coefficient (γ). By introducing a strain effect in the alloying system, the enhancement of MAE and γ were achieved. The alloying Fe/Cr can significantly change the electronic structure of the Fermi energy of Fe at Fe/MgO and hence modify MAE and γ . Additionally, we investigated the shape magnetic anisotropy energy (SMAE) in the ferromagnetic (FM) slabs, Fe/MgO, and antiferromagnetic (AFM) slabs MnX L1₀ structure (X: Pt, Ir, Pd, Ni). We found that a quadrupole component of Fe atomic spin density suppresses SMAE in ferromagnetic slabs with Fe/MgO interface. In the case of AFM MnPt slabs, which have a perpendicular favor originating from the crystalline magnetic dipole interaction, a surface effect at the Mn edge appears as an enhancement of SMAE.

Keywords: Magnetic anisotropy energy (MAE), alloying effect, strain effect, electric field effect, shape anisotropy, spin density functional theory (SDFT), spintronic applications.

1 Introduction

1.1 Research Background and Motivation

Magnetic anisotropy (MA) is one of the important properties of magnetic materials. MA quantifies the preferred orientation of magnetization i.e either perpendicular-to-plane or in-plane. Experimentally, MA is determined from the information provided by field dependent measurement along two orthogonal directions of the magnetic field relative to the sample. In bulk materials, MA relatively small, but it can markedly change in thin film or multilayer. This is due to the presence of symmetry breaking elements such as surfaces and interfaces.

Microscopically, there are two origins of MA. The first one is the magnetic dipolar interaction. Due to a long-range, the dipolar interaction generally result in shape-dependent contribution to the anisotropy, which is of particular importance in thin films and is largely responsible for the in-plane magnetization usually observed. This kind of origin can not explain the perpendicular MA (PMA). The second one is spin-orbit interaction. This origin can be interpreted as the coupling between the spin of the electron and the magnetic field created by its own orbital motion around the nucleus. As the orbital motion itself is directly coupled to the lattice via electric potential of the ion, this term provide a contribution to the magnetocrystalline anisotropy (MCAE).

The ability to grow a thin film nanostructure has lead to the materials with novel magnetic properties. At the nanoscale region, control of magnetization direction by magnetic field was demonstrated [1, 2] and a real application has been made as a magnetic storage hard disk drive (HDD). In the device magnetic memory, the building blocks made by a magnetic tunnel junction (MTJ). An MTJ consist of two ferromagnetic (FM) layer separated by insulator. Electrons can tunnel through the barrier and the tunneling amplitude depend on the relative angle of magnetization in each FM layer. This process called tunnel magnetoresistance (TMR) effect. The TMR ratio corresponds to the two resistance states. These two resistance states corespond to the "0" and "1" signals in memory devices. For the insulator layer, materials such as MgO are commonly used. This is due to the high TMR ratio. For FM layer, magnetic metal or alloys such as Fe, Co, Ni, Co/Ni, Co/Pd, Fe-Ga, FePt, FePd, CoFe, CoPd, NiFe, and CoFeB can be a choice. Nowadays, the magnetization orientation can be controlled by a current which can be lowering the energy consumption.

Although remarkable application has been achieved by controlling the magnetization, a remaining challenge to reduce power consumption still needed. Especially, the recent initiative in the internet of things (IoT), artificial intelligence (AI), big data, cloud computing, and advanced safety vehicle (ASV) which require a high density, high speed and low power storage device.

One of the solution to overcome this problem is using electric field (EF) instead of current. The new type of MRAM controlled by EF called Magnetoelectric (ME)-RAM. In the ME-RAM, EF can be generated by voltage, so unwanted energy consumption due to ohmic dissipation of the electric-current flow can be reduced. The voltage control magnetic anisotropy (VCMA) in a magnetic metal for the first time reported by Wesheit et al [3]. Inspired by this observation, a large number of experimental work and theoretical investigation on EF control magnetism has been devoted, driven both an urge to understand the mechanism and demand for better performance. The mechanism of VCMA here was discussed along with the charge-doping induced anisotropy changes [4].

Several early theoretical results also proposed the possible microscopic origin such as EF induce charge densities change on the surface of the film [5], EF induce change in band structure (p orbitals coupled to the d orbital) [6], and modification in the electron filling of each $3d$ orbital by EF, resulting in the accumulated charge at the magnetic layer [7]. Later, another theoretical group also proposed possible origin include a modulation of Rashba parameter [8, 9] and EF induced orbital hybridization changes.

The VCMA coefficient (the changes of MA respect to the EF) is one of the most important parameter in the design of ME-RAM. For example, in the case of PMA in the range of 0.6 mJ/m^2 to 1.5 mJ/m^2 , the required VCMA coefficients are in the range of 600 fJ/Vm to 1500 fJ/Vm . Due to this request, many efforts has been devoted from both experiments and theoretical sites. Since, the EF screen at the metal/oxide layer, so the most effective way to enhance the VCMA coefficient is to engineering the interface. But, at the same time, there are some disadvantages such as reducing the PMA and TMR ratio. Another choice is using alloying effect, underlayer effect and strain effect. Nozaki *et al* show that such alloying between Fe/Cr in the underlayer region of Cr/Fe/MgO structure, which possibly happens when an annealing is used during the deposition process, makes a large effect the quantities of PMA and VCMA coefficient. In this experiment, the PMA and VCMA coefficient reaches the value of 2.1 mJ/m^2 and 290 fJ/Vm . Recently, VCMA in antiferromagnetic (AFM) materials also reported [13, 14]. AFM materials with spin moments in antiparallel configuration produce no stray fields and insensitive the external magnetic field perturbations. Another advantage is ultrafast dynamics which ideal for future candidate memory storage, and spintronic applications [15].

Although large amount of significant works have been done in the area of VCMA, it is still a developing and energetic research topic and with a lot of open questions in fundamental mechanism, performances and practical applications of VCMA. Further experimental and theoretical investigations maybe strongly needed to accelerate the development of ME-RAM based on VCMA.

1.2 Research Objectives

Taking advantage of first principles approach associated with a deeper insight and an extended understanding of the underlying mechanisms of magnetic anisotropy and electric field effect on magnetic anisotropy, this research will focus on two main goals. The first goal of this work is to investigate the effect of the electric field, strain and alloying to the magnetic anisotropy energy (MAE) in metal/oxide heterostructure. The MAE originated from spin-orbit interaction and magnetic dipole interaction will be involved in the calculation. The possible origin of the enhancement of MAE and EF control MAE will be discussed with the detail of the electronic structure. The second goal is to investigate the shape magnetic anisotropy energy (SMAE) in the structure with ferromagnetic and antiferromagnetic spin magnetic configuration. In the evaluation of SMAE, several methods will be used and compared to each other.

2 Computational Method

In the first topic, we studied the MAE in Cr/Fe/MgO structure by introduce the Fe/Cr alloying. Such alloying is based on the suggestion from the experimental measurement [10]. An alloying of $[\text{Fe/Cr}]_n$ ($n=1,2$) has been considered. For $n=1$ and $n=2$, we called system-A and system-B, respectively. For a comparison, a structure without alloying also

considered (structure-I). The model structure for the calculation is shown in Fig. 1.

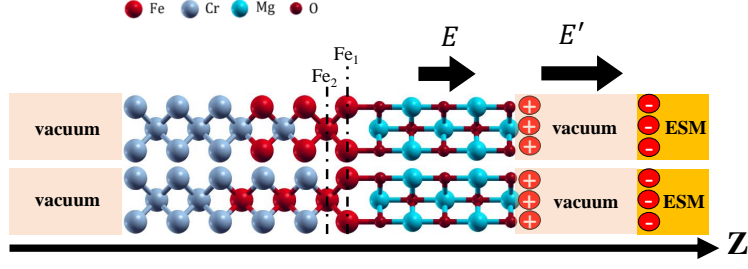


Figure 1: Schematic diagram of the computational model (a) system-A and (b) system-B. The black arrows with label E and E' indicate the electric field in MgO and the vacuum respectively.

In the calculation, we use spin density functional theory (SDFT) scheme implemented in house code [16], which employ scalar and fully relativistic ultrasoft pseudopotentials and planewave basis [17][18]. The generalized gradient approximation (GGA) for the exchange-correlation energy [19]. In the evaluation of MAE, we considered two kinds of contributions, namely magnetocrystalline anisotropy energy (MCAE) originated from spin-orbit coupling (SOC) and shape magnetic anisotropy energy (SMAE) originated from magnetic dipole-dipole interaction (MDI). The MCAE part was calculated based on the total energy (TE) and grand canonical force theorem (GCFT). In the GCFT scheme, we performed the atom-resolved and k -resolved contribution to MCAE. For SMAE contribution, we estimate by using the continuum approach (CA), discrete approach (DA) and spin density approach (SDA). In SDA approach, we evaluated the atomic multipole spin density such as quadrupole component [20]. To apply an EF, we used the effective screening medium (ESM) method [21]. The EF inside the MgO layer is estimated by we took into account the dielectric constant ϵ_r (9.8 for MgO).

2.1 Magnetic anisotropy energy

2.1.1 Total energy difference (TE)

In the presence of SOC, the total energy (TE) depends on the magnetization direction. The direction is denoted by $\hat{\mathbf{m}}$ (presented as [001], [100] or [010]). In this dissertation, we consider the MAEs of total energy difference, as follows:

$$\text{MAE} = E_{\text{tot}}^{[100]} - E_{\text{tot}}^{[001]} = \text{MCAE} + \text{MDIE}, \quad (1)$$

$$\text{MCAE} = E_{\text{SDFT}}^{[100]} - E_{\text{SDFT}}^{[001]}, \quad (2)$$

$$\text{MDIE} = E_{\text{MDI}}^{[100]} - E_{\text{MDI}}^{[001]}. \quad (3)$$

[001] indicate magnetization along z -direction and [100] indicates the magnetization along x -direction.

2.1.2 Grand-canonical force theorem

Alternatively, the MCAE can be estimated in a different procedure. That procedure is based on magnetic force theorem (FT) [11]. This approach has successfully been used in the evaluation of MAE, such as several cubic/tetragonal bulk systems. However, we need

an additional treatment for an accurate MAE of 2D or 1D system [12]. That is based on a grand-canonical force theorem (GCFT). In this dissertation, we take an approach similar to the GCFT.

In the GCFT scheme, the MCAE evaluated as,

$$\text{MCAE} = \sum_i f_i^{\hat{\mathbf{m}}_1} (\tilde{\varepsilon}_i^{\hat{\mathbf{m}}_1} - \mu) - \sum_i f_i^{\hat{\mathbf{m}}_2} (\tilde{\varepsilon}_i^{\hat{\mathbf{m}}_2} - \mu) \quad (4)$$

$$= \sum_i f_i^{\hat{\mathbf{m}}_1} \tilde{\varepsilon}_i^{\hat{\mathbf{m}}_1} - \sum_i f_i^{\hat{\mathbf{m}}_2} \tilde{\varepsilon}_i^{\hat{\mathbf{m}}_2} \quad (5)$$

where where $f_i^{\hat{\mathbf{m}}}$ and f_i^0 are electron occupations with and without SOC, and μ^0 is chemical potentials.

In order to separate the total MCAE to atom-resolved or \mathbf{k} -resolved contributions, we consider a total energy related to Eq. (4):

$$\delta E_{\text{SDFT}}^{\text{gf}, \hat{\mathbf{m}}} = \sum_i f_i^{\hat{\mathbf{m}}} (\tilde{\varepsilon}_i^{\hat{\mathbf{m}}} - \mu). \quad (6)$$

Using the explicit notation of $i = (n, \mathbf{k})$,

$$\delta E_{\text{SDFT}}^{\text{gf}, \hat{\mathbf{m}}}(\mathbf{k}) = \sum_n f_{n\mathbf{k}}^{\hat{\mathbf{m}}} (\tilde{\varepsilon}_{n\mathbf{k}}^{\hat{\mathbf{m}}} - \mu), \quad (7)$$

$$\delta E_{\text{SDFT}}^{\text{gf}, \hat{\mathbf{m}}}(I) = \sum_n \sum_{\mathbf{k}} \sum_a f_{n\mathbf{k}}^{\hat{\mathbf{m}}} (\tilde{\varepsilon}_{n\mathbf{k}}^{\hat{\mathbf{m}}} - \mu) |\langle \chi_{Ia} | \Phi_{n\mathbf{k}} \rangle|^2, \quad (8)$$

$$\delta E_{\text{SDFT}}^{\text{gf}, \hat{\mathbf{m}}}(I, \mathbf{k}) = \sum_n \sum_a f_{n\mathbf{k}}^{\hat{\mathbf{m}}} (\tilde{\varepsilon}_{n\mathbf{k}}^{\hat{\mathbf{m}}} - \mu) |\langle \chi_{Ia} | \Phi_{n\mathbf{k}} \rangle|^2, \quad (9)$$

where χ_{Ia} is the a 'th atomic orbital on the atom I . As indicated in Eqs. (7) – (9), the \mathbf{k} -resolved or atom-resolved contribution depends on μ and $f_{n\mathbf{k}}^{\hat{\mathbf{m}}}$ as well as $\tilde{\varepsilon}_{n\mathbf{k}}^{\hat{\mathbf{m}}}$. Both of the \mathbf{k} -space distribution $\delta E_{\text{SDFT}}^{\text{gf}, \hat{\mathbf{m}}}(\mathbf{k})$ and the atom distribution may be sensitive to μ . Nevertheless the main feature of these distributions may come from $\tilde{\varepsilon}_{n\mathbf{k}}^{\hat{\mathbf{m}}}$. Therefore, the \mathbf{k} -variation of $\delta E_{\text{SDFT}}^{\text{gf}, \hat{\mathbf{m}}}(\mathbf{k})$ will has a symmetry of system.

The \mathbf{k} -resolved or atom-resolved MCAE is given by the energy difference between the magnetization directions of $\hat{\mathbf{m}}_1$ and $\hat{\mathbf{m}}_2$ using Eq. (7) or Eq. (8):

$$\text{MCAE}(\mathbf{k}) = \delta E_{\text{SDFT}}^{\text{gf}, \hat{\mathbf{m}}_1}(\mathbf{k}) - \delta E_{\text{SDFT}}^{\text{gf}, \hat{\mathbf{m}}_2}(\mathbf{k}), \quad (10)$$

$$\text{MCAE}(I) = \delta E_{\text{SDFT}}^{\text{gf}, \hat{\mathbf{m}}_1}(I) - \delta E_{\text{SDFT}}^{\text{gf}, \hat{\mathbf{m}}_2}(I), \quad (11)$$

$$\text{MCAE}(I, \mathbf{k}) = \delta E_{\text{SDFT}}^{\text{gf}, \hat{\mathbf{m}}_1}(I, \mathbf{k}) - \delta E_{\text{SDFT}}^{\text{gf}, \hat{\mathbf{m}}_2}(I, \mathbf{k}). \quad (12)$$

In this dissertation, results for $\hat{\mathbf{m}}_2 = [001]$ and $\hat{\mathbf{m}}_1 = [100]$ will be presented.

3 Results and Discussions

3.1 Magnetic anisotropy energy at Fe/MgO interface

From TE calculation, the MCAE in system-A and system-B were largely enhanced compared to structure-I as summarized in Table. 1. After combined with the MDIE contribution, the perpendicular MAE (PMAE) was observed for system-A and system-B,

Table 1: The MAE from MCAE and MDIE for Cr(6MLs)/Fe(4MLs)/MgO(5MLs) (structure-I), system-A and system-B. The MCAE evaluated based on total energy (TE). The MDIE evaluated from discrete approach (DA) and spin density approach (SDA).

Structure	$a(\text{\AA})$	MCAE(SOI) mJ/m ²	MDIE mJ/m ²		MAE (SOI+MDIE) mJ/m ²	
			DA	SDA	SOI+DA	SOI+SDA
I	2.88	0.586	-1.353	-1.336	-0.763	-0.750
System-A	2.88	1.280	-1.097	-1.053	0.183	0.227
System-B	2.88	1.483	-0.829	-0.797	0.651	0.686

respectively, while for structure-I shows in-plane MAE (IMAE). The result in system-A and system-B has a qualitative agreement with MAE observed in experiment [10].

To elucidate the possible origin of the enhancement of MAE, we systematically analyzed the MCAE in GCFT scheme. At first, we confirm that the MCAE calculated from TE and GCFT has a good agreement. This agreement allow us for further analysis of atom resolved and k -resolved MCAE.

The atom resolved show that the main positive contribution to the MCAE is originated from (Fe₁). Furthermore, from k -resolved MCAE result, we can clearly see the region in two dimensional first Brillouin zone (2DBZ) which contribute to the positive and negative of MCAE as shown in Fig. 2.

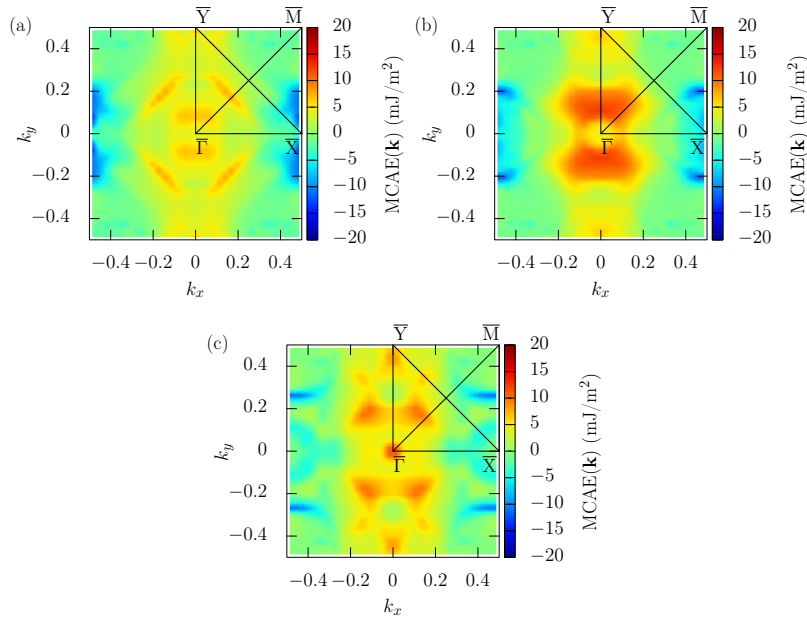


Figure 2: k -resolved MCAE, (a) Structure-I, (b) system-A, and (c) system-B, respectively.

Since total energy change (MCAE) which originated from SOC is very small, it can be treat as perturbation. Based on the perturbation theory, the change can be describe by considering up to second order term. Thus MCAE can be written as,

$$\text{MCAE} \approx \xi^2 \sum_{\mathbf{k}_o, \mathbf{k}_u} \frac{|\langle \mathbf{k}_o | \hat{\ell}_z | \mathbf{k}_u \rangle|^2 - |\langle \mathbf{k}_o | \hat{\ell}_x | \mathbf{k}_u \rangle|^2}{\varepsilon_{\mathbf{k}_u} - \varepsilon_{\mathbf{k}_o}}, \quad (13)$$

where \mathbf{k}_o and \mathbf{k}_u indicate the occupied and unoccupied states with the wave vector \mathbf{k} and \hat{l}_z, \hat{l}_x are the angular momentum operators. $\varepsilon_{\mathbf{k}u}$ and $\varepsilon_{\mathbf{k}o}$ indicate the energies of unoccupied and occupied states. The SOC between occupied and unoccupied state with the same (different) in magnetic quantum number through to the \hat{l}_z (\hat{l}_x and \hat{l}_y) operators give positive (negative) contribution to MCAE

Based on the analysis of Eq. 13, we found that, the positive and negative region in 2DBZ is strongly related to the pair d -orbital coupling near the Fermi energy. By introducing alloying, there is a remarkable changes in the electronic structure. For $n=2$, the d -orbital states become more localized, and hence can modify the MCAE.

Next, we calculated the electric field (EF) effect for system-A and system-B. We observed an opposite sign of MCAE coefficient (γ), which is positive and negative for system-A and system-B, respectively as shown in Fig. 3.

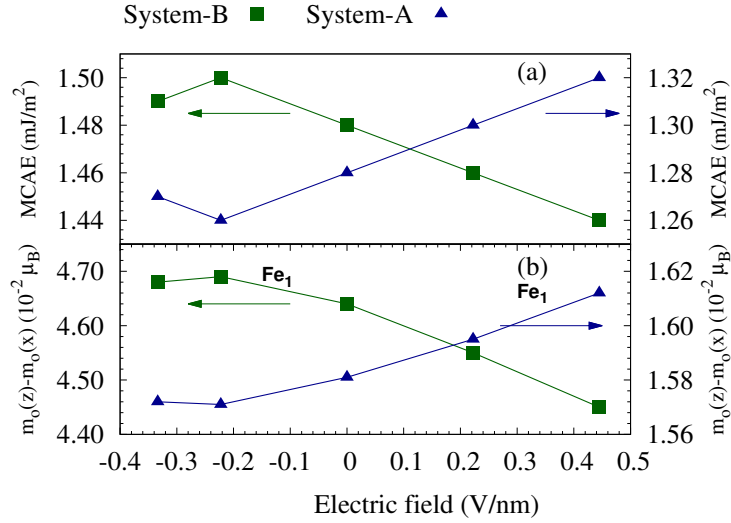


Figure 3: (a) MCAE and (b) orbital moment differences as EF dependence in system A (blue triangles) and system B (red squares).

The orbital moment and band filling calculation also show the same behavior. From atomic resolved analysis, we found that MCAE changes by EF mainly observed at (Fe_1). Moreover, from different of k -resolved MCAE at zero and with EF ($\Delta MCA(k)$), we can clearly see that as final result show a positive for system-A, while negative for system-B.

The enhancement of MCAE and opposite sign in γ may related to the impact of Fe/Cr alloying which make a remarkable changes in the electronic structure, especially Fe interface with MgO (Fe_1). Here, we addressed such changes may related to the proximity effect of Fe and Cr. The proximity effect here is associated with two mechanisms. At first, the hybridization with Cr: Fe d -states are shifted to the lower energy since Cr d -states are located in the higher energy [22]. At second, electrons can transfer from Cr to Fe atoms due to a smaller electronegativity of Cr. Consequently, the number of $3d$ electrons on the Fe of Fe/MgO interface may increase. This increase strongly depends on the vicinity of Cr next to Fe/MgO interface. In addition, we also observe that the number of electrons (NOE) in d -orbital for system-B is increased by 0.052 from that for system-A. This larger NOE may be an origin of sign change in γ . Experimentally, an opposite sign in voltage control magnetic anisotropy (VCMA) was also observed between Ta and Ru underlayers. Discussion of this opposite sign was related to a different spin-orbit coupling in the underlayer, a difference in crystallinity etc., but the origin is still an open question

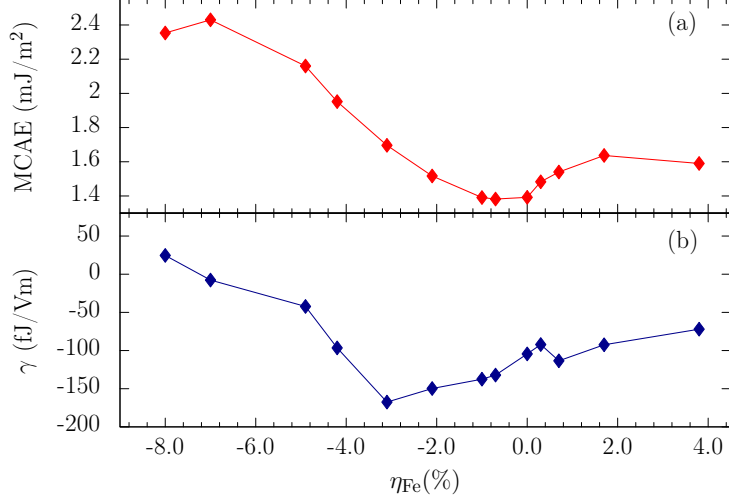


Figure 4: (a) MCAE and (b) electric-field induced MCAE coefficient (γ) in system B as strain dependence.

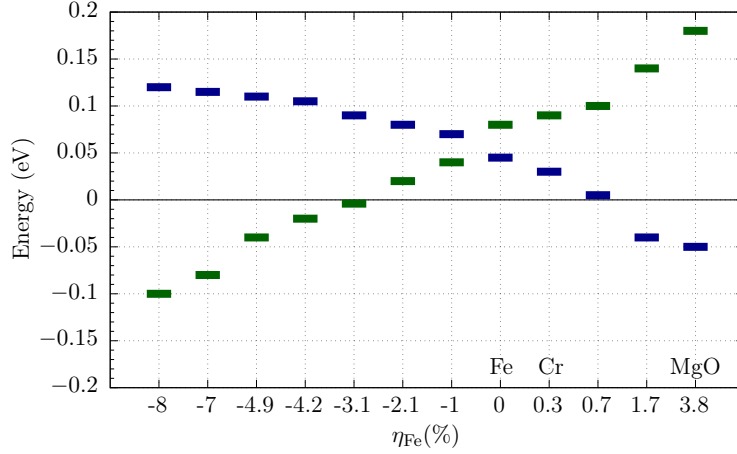


Figure 5: Energy of minority orbitals $d_{x^2-y^2}$ (green) and d_{xy} (blue) along the $\bar{X}-\bar{Y}$ line for Fe at Fe/MgO interface.

[23].

In the vicinity of the Fermi energy, we calculate the MCAE in system-B as strain dependence with respect to the Fe lattice constant (η_{Fe}). The MCAE increases with the increasing tensile strain (increase in lattice constant) and increasing compressive strain (reduce in lattice constant) with the maximum value of 2.43 mJ/m² at $\eta_{\text{Fe}} = 2\%$ as shown in Fig. 4(a).

To elucidate the possible origin, we systematically analyzed the k -resolved MCAE and compared with the electronic structure. We notice that the behavior of MCAE as strain dependence may related to the pair coupling of $d_{x^2-y^2}$ and d_{xy} along the $\bar{X}-\bar{Y}$ line as shown in the Fig. 5.

Furthermore, larger MCAE at $\eta_{\text{Fe}} = -7\%$ may related to the large amount of state in the Fermi energy and suitable pair coupling which promote to the PMCAE. In addition, based on atomic resolved MCAE, we found that, by introduce compressive strain, the Fe inside the layer also contribute the PMCAE. Next, we calculated the EF effect on MCAE for each strain condition. The results are shown in Fig. 4(b). The maximum value of $\gamma=170$ fJ/Vm was achieved at $\eta_{\text{Fe}} = -3.1\%$. Larger γ at $\eta_{\text{Fe}} = -3.1\%$ is related to the

large amount of d -orbital states (d_{xz} , d_{yz} , $d_{x^2-y^2}$, d_{xy}) along the \bar{X} - \bar{Y} line. As result, small change in orbital occupation induce by EF, may significantly changes the MCAE.

3.2 Shape Magnetic Anisotropy From Spin Density in Nanoscale Slab Systems

For the second topic, we systematically investigate the SMAE in ferromagnetic (FM) slabs Fe, Fe/MgO and antiferromagnetic (AFM) MnX L1₀ structure (X: Pt, Ir, Pd, Ni). In the calculation, we consider model of MgO(5ML)/Fe(x ML)/MgO(5ML) ($x=110$) slab with the in-plane lattice constant extracted from MgO. This slab has vacuum layers of 0.9 nm thick on both the sides of the layer. After the relaxation of layer distances, we estimated the SMAEs for CA, DA, and SDA. The midpoint-to-midpoint layer distance between the Fe/MgO interfaces was taken as layer thickness. In order to identify the difference between the surface and interface effects, we also evaluated the MAE of a Fe(x ML) slab obtained by deleting the MgO layers from the MgO/Fe(x ML)/MgO slabs. For MnX slabs (X=Pt, Ir, Pd, and Ni), the structure extracted from the bulk with L1₀ ordered alloy. Assuming that an antiferromagnetic configuration is the same as in the bulk, where the total magnetization in the same Mn-atom layer vanishes and the atomic magnetic moments are parallel to those of the nearest-neighboring Mn layers. In the evaluations of EDA and ESDA, a $\sqrt{2} \times \sqrt{2}$ magnetic unit cell was taken for an in-plane periodicity with the lattice constant of 7.56 Bohr, 7.28 Bohr, 7.69 Bohr, 7.07 Bohr for MnPt, MnIr, MnPd, and MnNi, respectively.

In the case of FM Fe and Fe/MgO interface, there is a reduction of E_{CA} compared to the E_{DA} and E_{SDA} as shown in the Fig. 6.

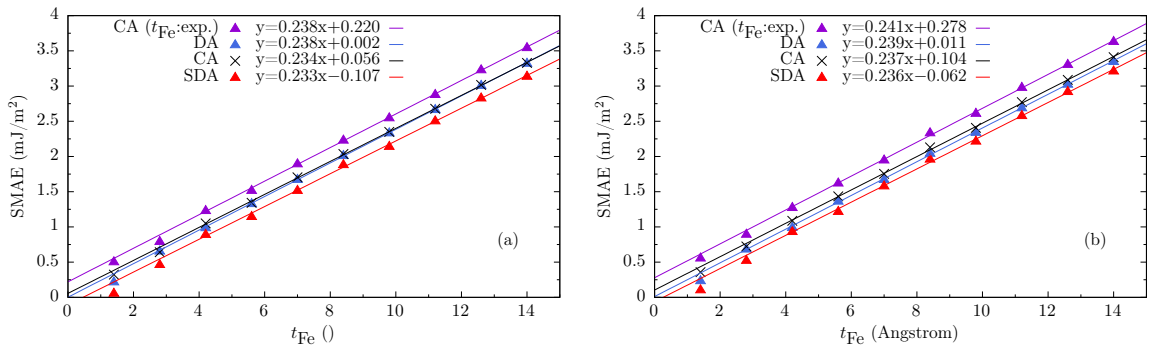


Figure 6: SMAE of (a) MgO/Fe(x ML)/MgO and (b) Fe(x ML) ($x=110$) for CA, DA, and SDA. The CA with the experimental thickness (0.14 nm/FeML) is also plotted. The lines are deduced from the least square fitting using the data of $x=3-10$.

This reduction is originated from quadrupole component of Fe at the surface and Fe at the interface. Such quadrupole component show a prolate shape density distribution as shown in Fig. 7(a) and (b) for Fe/MgO and Fe, respectively. On the inside, the quadrupole component is reduced significantly compared with that on the interface. In addition, from Fig. Fig. 7(a) and (b), we can see that MgO/Fe(x ML)/MgO has larger quadrupole component compare to the Fe(x ML). As a result, the reduction of SMAE(SDA) from SMAE(CA) in MgO/Fe(x ML)/MgO become larger.

On the other hand, in the case of AFM MnX (X: Pt, Ir, Pd, Ni), the quadrupole component of Mn at surface contribute to the enhancement of SMAE. The difference of E_{DA} and E_{SDA} originating from the quadrupole component on Mn atom inside layer.

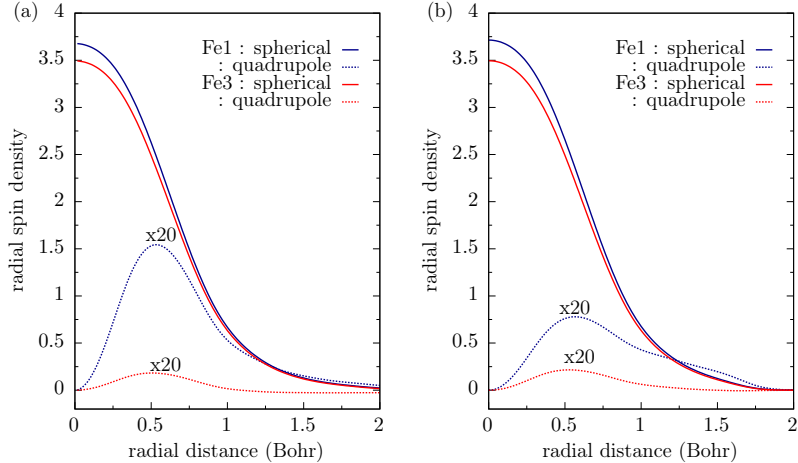


Figure 7: Radial atomic spin density distribution [in(Bohr)³] in (a) MgO/Fe(5ML)/MgO and (b) Fe(5ML). Fe1 indicate the interface/surface atoms, and Fe3 indicate the atoms inside the layer. All the quadrupole components are magnified 20 times.

Furthermore, the bulk property of SMAE estimated from the slope of the fitted line E_{SDA} result has a good agreement with SDA calculation of bulk structure as shown in Table. 2.

Table 2: The MAE of bulk antiferromagnetic MnX systems (X: Pt, Ir, Pd, Ni). The MDIE evaluated from spin density approach (SDA).

System	$a(\text{\AA})$	c/a	MAE (meV/cell)		MAE(SOI) (meV/cell) [24]
			SOI	SDA	
MnPt	3.990	0.927	0.150	0.186	0.510
MnIr	3.885	0.945	-8.204	0.105	-7.050
MnPd	4.070	0.880	-0.419	0.218	-0.570
MnNi	3.740	0.941	-0.448	0.202	-0.290

4 Conclusions

In conclusion for the first topic, we found that introducing alloying Fe/Cr can promote the perpendicular MAE (PMAE) in Cr/Fe/MgO structure. Furthermore, different alloying conditions can lead to the opposite change in EF coefficient (γ). The alloying effect can induce a substantial rearrangement in the electronic structure due to the proximity effects of Fe and Cr. The proximity effect here is associated with Cr-Fe hybridization and electrons transfer from Cr to Fe atoms due to smaller electronegativity of Cr. Consequently, the number of $3d$ electrons on the Fe at Fe/MgO interface may increase. By introducing a strain effect in the alloying system, the enhancement of MAE and γ were achieved. From the atom resolved calculation, we found that the positive contribution to the MCAE mainly comes from Fe at Fe/MgO interface. And also, from k -resolved MCAE result, we found that positive and negative contribution observes only at certain regions in the two-dimensional first Brillouin zone. That contribution can be related to the cer-

tain pair coupling of states between the Fermi energy by considering the second-order perturbation theory.

For the second topic, we found that a quadrupole component of Fe atomic spin density suppresses SMAE in ferromagnetic slabs with Fe/MgO interface. In antiferromagnetic MnPt slabs, which have a perpendicular favor originating from the crystalline magnetic dipole interaction, a surface effect at the Mn edge appears as an enhancement of SMAE.

References

- [1] M. N. Baibich et. al., Phys. Rev. Lett. 61, 2472 (1988).
- [2] G. Binasch et. al., Phys. Rev. B 39, 4828 (1989)
- [3] M. Weisheit et, al., Science 315(5810), 349 (2007).
- [4] T. Maruyama et. al., Nature Nanotechnology 4(3) (2009).
- [5] Chun-Gang Duan, et. al., Phys. Rev. Lett. 101, 137201 (2008).
- [6] K. Nakamura et. al., Phys. Rev. Lett. 102, 187201 (2009).
- [7] M. Tsujikawa and T. Oda, Phys. Rev. Lett. 102:247203, (2009).
- [8] L. Xu and S. Zhang, J. Appl. Phys. 111(7), 2012 (2012).
- [9] S. E. Barnes et. al., Scientific Reports. 4, 1 (2014).
- [10] T. Nozaki et. all., Phys. Rev. Applied. 5, 044006 (2016).
- [11] G. H. O. Daalderop et. all., Phys. Rev. B 41, 11919 (1990).
- [12] D. Li et. all., Phys. Rev. B 88:214413, (2013).
- [13] M. Goto et. al., Jpn. J. Appl. Phys. 55(8), 080304 (2016).
- [14] Y. Wang et. al., Advanced Materials 27(20), 3196(2015).
- [15] S. Loth et, al., Science 335(6065), 196 (2012).
- [16] T. Oda et. al., Phys. Rev. Lett. 80(16), 3622 (1998).
- [17] K. Laasonen at. al., Phys. Rev. B 47, 10142 (1993).
- [18] T. Oda and A. Hosokawa, Phys. Rev. B 72, 224428 (2005).
- [19] J. P. Perdew et. al., Phys. Rev. B 46, 6671, 1992.
- [20] T. Oda and M. Obata, J. Phys. Soc. Jpn. 87(6), 064803, (2018).
- [21] M. Otani and O. Sugino, Phys. Rev. B 73, 115407 (2006).
- [22] M. Ogura et. al., J. Phys. Soc. Jpn. 80(10), 1 (2011).
- [23] Y. Shiota et. al., Appl. Phys. Lett. 103(8) (2013).
- [24] R. Y. Umetsu, A. Sakuma, and K. Fukamichi., Appl. Phys. Lett. 89, 052504 (2006)

学位論文審査報告書（甲）

1. 学位論文題目（外国語の場合は和訳を付けること。）

First-principles design of magnetic anisotropy in nanostructures by electric-field, strain, and metal alloying (和訳：電界、ひずみ、合金化によるナノ構造磁気異方性の第一原理設計)

2. 論文提出者 (1) 所属 数物科学 専攻

(2) 氏名 ばるでで いんどら Pardede Indra

3. 審査結果の要旨（600～650字）

...Pardede Indra 氏の提出論文について、各審査委員が個別に検討し、予備審査会の後、詳細に検討した。令和元年7月30日に開催された公聴会(口頭発表)の後に、審査委員会を開催し、協議の結果以下のように判定した。

...Pardede 氏は、密度汎関数法に基づいた第一原理電子状態計算(非経験的電子構造計算)を用いて、面直磁気異方性を示す Fe/MgO 界面をもつ薄膜系について、磁気異方性エネルギー(MAE)等の磁気的特性を計算し、磁気メモリ素子を構成し得る材料の設計指針を検討した。用いた計算手法は、MAE 等の特性について予測能力の高いものであり、電界印加が可能なものである。彼は、下地金属層(Cr)/強磁性金属層(Fe)/酸化物絶縁層(MgO)等のスラブ系を中心に計算を推進し、MAE に対する電界効果、CrFe 合金化効果、面内歪効果を詳細に調査した。彼は合金化によりスラブ系全体で面直磁気異方性を高めること、電界効果の符号が反転することを示した。また、面内歪により面直磁気異方性を高める歪量や電界効果が最大となる歪量を明らかにした。得られた計算結果や設計指針は、電圧駆動型磁気メモリ素子の開発を加速し、磁性界面研究に貢献するものである。以上の成果をまとめた本論文は、博士(理学)の学位に値するものと判定した。

4. 審査結果 (1) 判定 (いずれかに○印) 合格 ・ 不合格
(2) 授与学位 博士(理学)